doi: 10.56761/EFRE2024.C4-O-060601

Surface plasma modifications of UFG magnesium alloy

K.A. Prosolov[1,], V.V. Lastovka[1], N.A. Luginin[1,2], M.A. Khimich[1], A.D. Kashin[1], A.U. Eroshenko[1], M.B. Sedelnikova[1], Yu.P. Sharkeev[1,2]*

[1]*Institute of Strength Physics and Materials Science of SB RAS, Tomsk, Russia*
[2]*National Research Tomsk Polytechnic University, Tomsk, Russia*
[*]*konstprosolov@gmail.com*

Abstract. Development of new biodegradable composite material is of key importance for modern healthcare. We propose **s**urface plasma modifications of ultrafine-grained (UFG) magnesium alloys to enhance their potential for biomedical applications. UFG magnesium alloys, despite their favorable mechanical properties and biocompatibility, suffer from rapid corrosion in physiological environments. To address this issue, we deposited strontium-doped calcium phosphate (Sr-CaP) coatings on UFG magnesium substrates. Additionally, zirconium dioxide (ZrO_2) or titanium dioxide (TiO_2) coatings were deposited on top of the Sr-CaP layers to further improve corrosion resistance, mechanical stability, and biological performance. Results indicated that ZrO_2 and TiO_2 top layers significantly enhanced the corrosion resistance and mechanical integrity of the Sr-CaP coated UFG magnesium alloys. The optimized coating parameters, including RF power, target-substrate distance, and working gas pressure, were established to achieve the desired coating morphology and composition. The study concludes that the multi-layered coating system comprising Sr-CaP with ZrO_2 or TiO_2 top layers provides a promising surface modification strategy for UFG magnesium alloys, making them suitable for use in medical implants.

Keywords: ultrafine-grained magnesium, biomedical implants, RF magnetron sputtering, corrosion.

1. Introduction

Ultrafine-grained (UFG) magnesium alloys have garnered significant attention in the biomedical field due to their excellent biocompatibility, biodegradability, and mechanical properties that closely resemble those of natural bone [1, 2]. However, their high corrosion rate in physiological environments poses a significant challenge for their practical application in medical implants [3]. To address this issue, surface modifications are crucial to enhance the corrosion resistance and biocompatibility of UFG magnesium alloys [4].

One promising approach to improve the surface properties of UFG magnesium alloys is the deposition of bioactive coatings. Among these, calcium phosphate (CaP) coatings, particularly those doped with strontium (Sr), have shown potential due to their ability to promote osteointegration and enhance bone formation [5]. Sr-doped CaP coatings combine the osteogenic properties of calcium phosphate with the beneficial effects of strontium, such as stimulating bone formation and inhibiting bone resorption [6]. These coatings not only act as a barrier to corrosion but also actively participate in the biological processes of bone regeneration [7].

Despite the advantages offered by Sr-doped CaP coatings, further improvements in coating performance are necessary to ensure long-term stability and functionality of the implants [8]. In this context, the application of an additional protective layer over the CaP coatings can significantly enhance their properties. Zirconium dioxide (ZrO_2) and titanium dioxide (TiO_2) are two materials that have been extensively studied for their excellent biocompatibility, high corrosion resistance, and favorable mechanical properties [9, 10]. These materials, when used as top coatings, can provide a robust protective barrier, thereby enhancing the overall performance of the underlying Sr-doped CaP coatings [11].

The deposition of ZrO_2 or TiO_2 coatings on top of Sr-doped CaP coatings on UFG magnesium alloys is a novel strategy aimed at achieving multiple objectives. Firstly, these top coatings can further enhance the corrosion resistance of the underlying magnesium alloy, thereby prolonging the lifespan of the implant in the physiological environment. Secondly, ZrO_2 and TiO_2 coatings can improve the mechanical stability of the coating system, ensuring that the implant can withstand the mechanical

stresses encountered in the body. Thirdly, these coatings can offer additional biological benefits, such as antibacterial properties and enhanced osteogenic potential, which are critical for the successful integration of the implant with the surrounding bone tissue.

The primary goal of this research is to investigate the effectiveness of ZrO_2 and TiO_2 coatings deposited on Sr-doped CaP coatings on UFG magnesium alloys for biomedical applications.

2. Materials and methods

A magnesium alloy MA-20 (Mg-Zn-Ce-Zr) from VIAM, Moscow, Russia, was used as the substrate material. The alloy's chemical composition was: Mg – 98.5%, Zn – 1.3%, Ce – 0.1%, and Zr – 0.1%. A combined severe plastic deformation technique produced MA-20spd with a fine-grained structure. The metal samples were pretreated through abrasive grinding with 400 and 600-grit sandpaper, achieving a roughness of 0.5–0.6 μm. After machining, the samples were treated in an ultrasonic cleaner (Elmasonic S, Elma, Germany) in distilled water and ethanol, followed by air drying. The coatings were produced by the micro-arc oxidation (MAO) method using an electrolyte suspension containing NaOH, Na_2SiO_3, NaF, and Sr(2.5)-hydroxyapatite $Ca_{7.5}Sr_{2.5}(PO_4)_6(OH)_2$ (Sr-HrA), prepared via a mechanochemical method at the Institute of Solid State Chemistry and Mechanochemistry, Siberian Branch of the RAS in Novosibirsk, Russia. The Sr-CP coatings were deposited in the anodic potentiostatic mode using MicroArc 3.0 equipment. The MAO process parameters were: duration of 5 and 10 minutes, pulse frequency of 50 Hz, pulse duration of 100 μs, and voltage varied from 350 to 500 V.

To study sputtering processes, two targets were prepared. The first was made from commercially pure titanium with a thickness of 3 mm, and the second from ZrO_2 with a thickness of 6 mm. Producing ceramic targets of small thickness posed technological challenges, so increased thickness was used, which may reduce sputtering efficiency due to disruption of the electron trap efficiency formed by magnetic induction lines on the target surface. An RF (13.56 MHz) magnetron system was employed to deposit CaP coatings, equipped with a 2.5 kW RF power supply (COMDEL CX-2500S, Gloucester, MA, USA) and an automatic matching network (COMDEL Match pro CPMX-2500, Gloucester, MA, USA). Deposition was conducted in a vacuum chamber with Ar as the operational gas, maintained at a constant pressure with a gas flow meter.

Coating thickness was determined via ellipsometry on monocrystalline Si samples, using an ELLIPS-1891 SAG spectral ellipsometric complex (SPC “Nanotechnology center”, Novosibirsk, Russia). Sputtering processes were studied by examining the spectral characteristics of the high-frequency plasma of a gas discharge, using an AvaSpec-2048-x-DT spectrometer, with a resolution accuracy of 0.2 nm in the range of 300 to 800 nm. OriginPro software was used to analyze and process the spectrograms. Scanning electron microscopy was conducted using a LEO EVO 50 electron microscope (Carl Zeiss AG, Germany) equipped with an INCA X-Act energy-dispersive X-ray spectroscope (Oxford Instruments, UK). The structural analysis of the coatings was conducted via X-ray diffraction (XRD) using a DRON-8H diffractometer (Bourevestnik, St. Petersburg, Russia). This instrument operated in the range of angles 2θ = 10–100°, with a scanning step of 0.02° in Cu-Kα radiation.

3. Results and discussion

Figure 1 presents the obtained spectra of the RF argon discharge produced during the sputtering of the ZrO_2 target material. Based on data from the NIST Atomic Spectra Database, The main emission lines of zirconium (Zr), oxygen (O), and argon (Ar) in the plasma discharge. These lines represent the wavelengths of emitted light that are most intense and typically observed for these elements under plasma conditions.

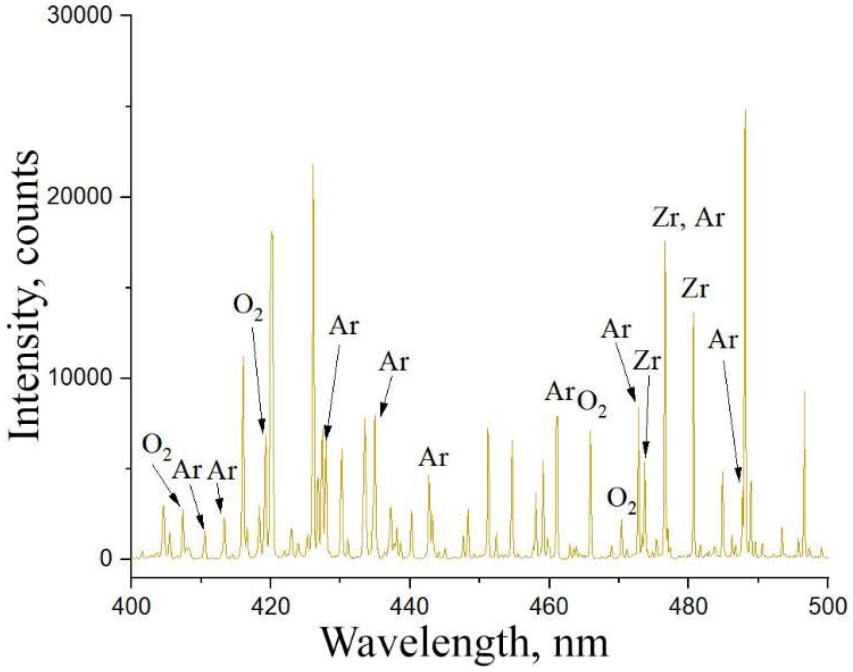

Fig. 1. RF magnetron discharge spectra for ZrO_2 target at working parameters RF power 300 W, pressure Ar 1.0 Pa.

The intensity of spectral lines in optical emission spectroscopy (OES) during RF sputtering changes with variations in RF power due to complex interactions between the plasma and the target. Several factors contribute to this increase in intensity. As the RF power increases from 50 to 300 W, the plasma energy rises. This additional energy results in more frequent and energetic collisions between electrons and gas atoms/molecules in the plasma. The increased frequency and energy of collisions lead to a higher rate of ionization of argon gas and sputtered oxygen and zirconium atoms. Greater ionization means more ions and excited particles emitting light at their characteristic wavelengths, resulting in an increase in the intensity of their spectral lines.

It is worth noting that in the spectra presented in Figure 1, the primary elements are Ar and O ions; Zr is ionized to a lesser extent and is mainly represented by neutrals. Increasing the RF power also results in more efficient sputtering as more energy is transferred to the target by Ar ion bombardment. This process can increase the amount of sputtered neutrals (e.g., Zr atoms) and ions (e.g., O from ZrO_2) in the plasma, contributing to the increased intensity of the associated spectral lines. Increasing the argon pressure from 0.1 Pa to 1 Pa in the RF sputtering system leads to significant changes in plasma characteristics and, consequently, the spectral lines observed during OES. Higher pressure leads to changes in temperature and electron density in the plasma. Depending on the RF power, this can increase the intensity of certain lines.

The growth rate was determined by the ellipsometric method on witness samples made of Si. The dependence of the growth rate on the applied RF power for Ti and ZrO_2 targets is presented in Figure 2. As shown in the graph, the deposition rate of ZrO_2 coatings is significantly higher than that of Ti at the selected power levels.

The selected distance did not fully ensure the required temperature regime on the surface of the substrates (no more than 50 °C), which was assessed by a chromel-alumel thermocouple after completion of the deposition process. At a power of 300 W, the temperature ranged from 63 to 71 °C.

The elemental composition of the formed coatings at different powers is presented in Figure 3. As shown in the bar diagram, the films closest to stoichiometric ZrO_2 were obtained at power levels of 250–300 W. It is also worth noting that at low power values, the concentration of Zr in the films remains low, which is consistent with previous studies on the intensity of Zr lines during OES.

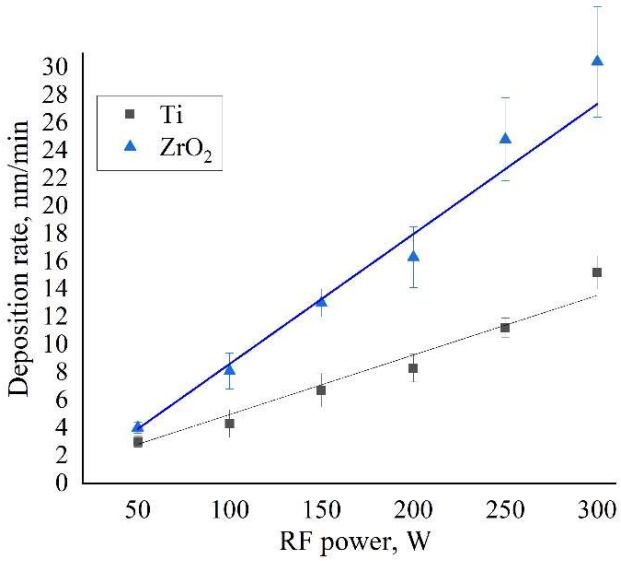

Fig. 2. Coating deposition rate on a Si substrate depending on the applied RF power. The distance from the target to the substrate is 100 mm.

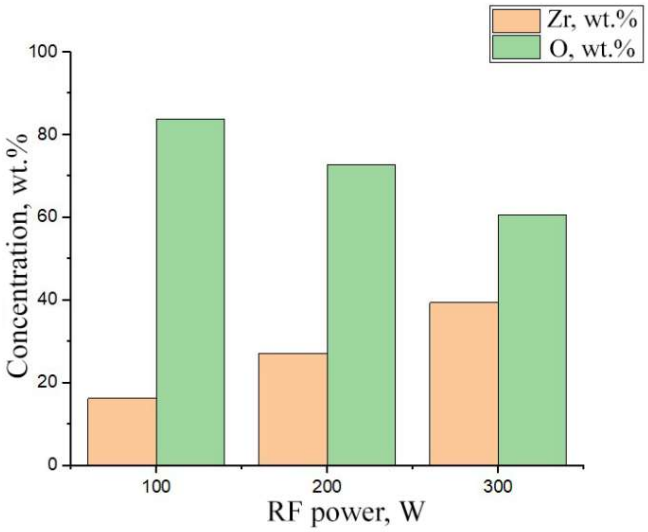

Fig. 3. Elemental composition of the formed coatings at different sputtering powers.

The morphology of Zr-containing coatings, according to SEM results, is represented by a dense layer with a core-type structure (Figure 4). The morphology of the cross section indicates weak crystallinity of the formed layers. To clarify the structural state, the X-ray diffraction method was used, and the results are presented in Figure 5. As shown, the main phase in all deposited coatings is zirconium dioxide (ZrO_2) in the monoclinic modification. All observed reflections are broadened and their intensity is reduced, indicating the small size of the formed structural elements and a high level of residual stresses in the structural elements of the main phase. In the diffraction patterns of coatings obtained at lower power, a second-order X-ray reflection line from the (100) plane of the substrate phase (Si) is clearly observed. This occurs because, at an RF power of 150 W, the thickness of the deposited coating is less than that at an RF power of 300 W, given the same deposition time and working gas pressure, which makes the reflections of the single-crystalline substrate visible in the diffraction pattern.

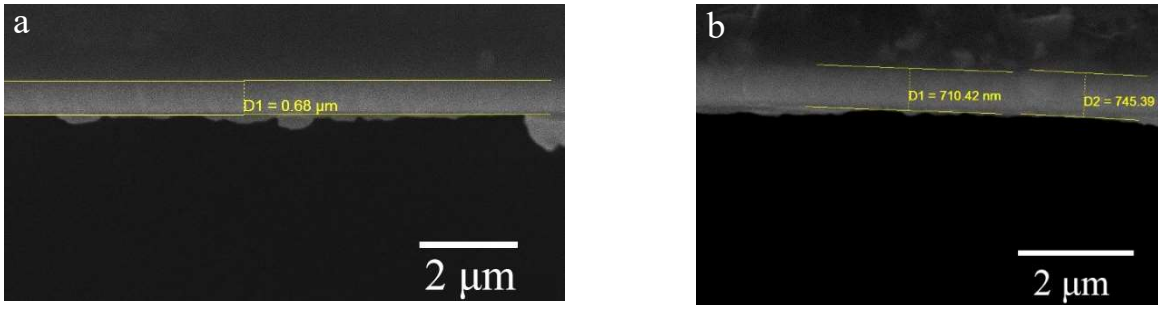

Fig. 4. SEM images of the morphology of Zr-containing coatings deposited at 300W (a) and 250 W (b).

As you can see, in all deposited coatings the main phase is zirconium dioxide ZrO_2 in the monoclinic modification (Figure 5). All observed reflections are broadened and their intensity is reduced, which indicates the small size of the formed structural elements, as well as a high level of residual stresses in the structural elements of the main phase. In the diffraction patterns of coatings obtained at lower power, a second-order X-ray reflection line from the (100) plane of the substrate phase (Si) is clearly observed. This is due to the fact that at an RF power of 150 W, the thickness of the deposited coating is less than in the case of an RF power of 300 W, subject to the same deposition time and working gas pressure, due to which the reflections of the single-crystalline substrate become visible in the diffraction pattern.

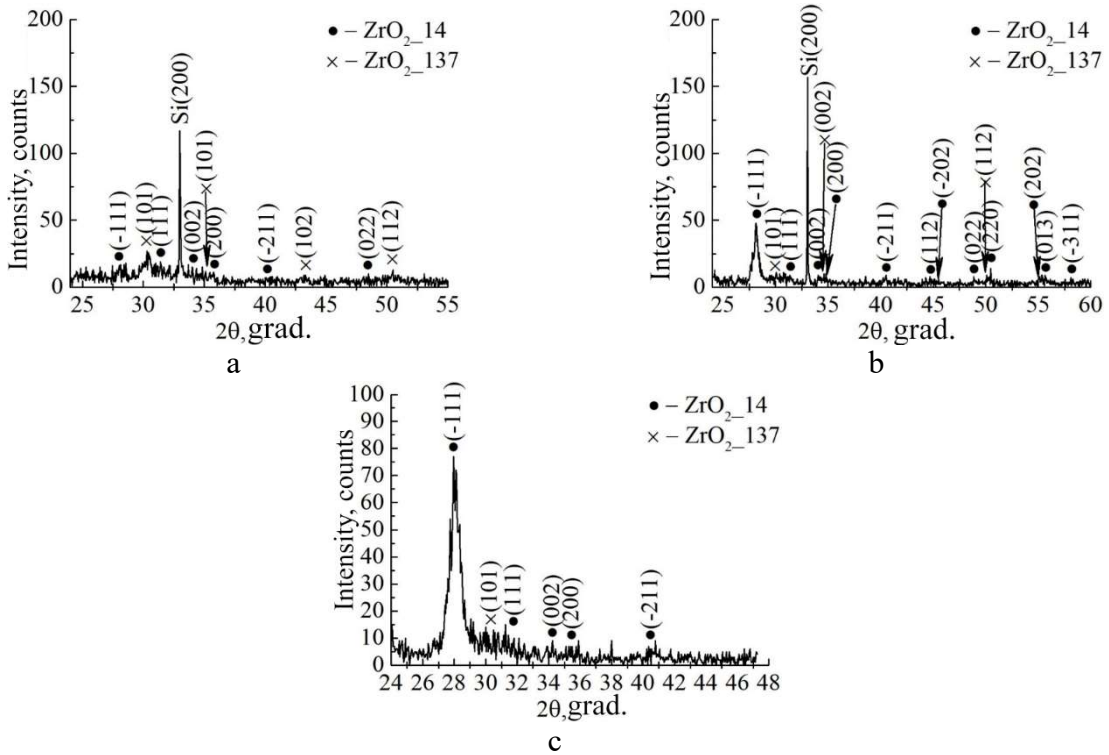

Fig. 5. X-ray diffraction of coatings sputtered from ZrO_2 target in different RF modes: power 150 W and pressure 0.1 Pa (a), 150 W and 1 Pa (b), 300 W and 0.1 Pa (c).

It can be seen that changes in the power and pressure of the working gas (Figure 5) affect the phase composition of the coating: at an RF power of 300 W and a pressure of 0.1 Pa, the phase composition of the coating is represented by a phase of monoclinic ZrO_2 and trace amounts of ZrO_2 in the tetragonal modification. With decreasing power and increasing working gas pressure, the volume fraction of tetragonal ZrO_2 increases (Figure 5a).

4. Conclusion

In this study, we explored the surface plasma modifications of UFG magnesium alloy to enhance its applicability in medical applications. The focus was on the structure, morphology, and composition of coatings. We can conclude that it is possible to deposit ZrO_2 or TiO_2 layers in different crystallinity states including on top of Sr-CaP coating and therefore improve electrochemical and mechanical properties of the composite that is, to our knowledge, have not been reported previously.

Acknowledgement

The work was financially supported by Russian Science Foundation, grant No. 23-13-00359.

5. References

[1] J.H. Jo, J.Y. Hong, K.S. Shin, H.E. Kim, and Y.H. Koh, Enhancing biocompatibility and corrosion resistance of Mg implants via surface treatments, *Journal of Biomaterials Application*, vol. **27**(4), 469–476, November 2012, doi: 10.1177/0885328211412633.

[2] Y. Yang, et al., Recent advances in magnesium alloys for biomedical applications, *Materials Science and Engineering: C*, vol. **78**, 1165–1175, 2017.

[3] A. Atrens, et al., Reviewing the current status of magnesium implants for biomedical applications: outcomes and challenges, *Acta Biomaterialia*, vol. **48**, 1–16, 2017.

[4] Y. Chen, et al., Magnesium-based alloys for biomedical applications: a review on corrosion, biocompatibility, and surface modifications, *Journal of Materials Science & Technology*, vol. **35**(10), 1999–2007, 2019.

[5] X. Luo, et al., Strontium-doped calcium phosphate coatings on magnesium substrates for improved biocompatibility and corrosion resistance, *Surface and Coatings Technology*, vol. **366**, 182–192, 2019.

[6] H. Zreiqat, et al., Strontium- and zinc-doped bioceramics promote human osteoblast activity and new bone formation, *Journal of Biomedical Materials Research Part A*, vol. **89A**(4), 1143–1152, 2009.

[7] X. Wang, et al., Strontium-containing hydroxyapatite coatings on magnesium alloys for improved corrosion resistance and biological performance, *Journal of Biomedical Materials Research Part B: Applied Biomaterials*, vol. **107**(4), 1185–1196, 2019.

[8] Y. Ding, et al., Innovative Bioceramic Coatings to Improve the Corrosion Resistance and Biocompatibility of Magnesium Implants, *Advanced Healthcare Materials*, vol. **7**(23), 1800497, 2018.

[9] A. Balamurugan, et al., Strontium-substituted hydroxyapatite (Sr-HA) nano powders synthesized by microwave processing: A study on the physicochemical properties and in vitro bioactivity, *Journal of Materials Science: Materials in Medicine*, vol. **19**, 1727–1736, 2008.

[10] H. Cao, et al., Bioactivity and osteogenic differentiation of TiO2 nanotubes surface coated with calcium phosphate by ion beam-assisted deposition, *Colloids and Surfaces B: Biointerfaces*, vol. **145**, 338–345, 2016.

[11] Revathi A., et al., Microstructure, mechanical properties, corrosion resistance and in vitro bioactivity of hydroxyapatite/zirconia composite coatings on magnesium by pulsed electrodeposition, *Materials Science and Engineering: C*, vol. **100**, 676–689, 2019.